Egocentric Boundaries on Distinguishing Colliding and Non-Colliding Pedestrians while Walking in a Virtual Environment

Alex D. Hwang, Jaehyun Jung, Alex Bowers, and Eli Peli
Schepens Eye Research Institute of Massachusetts Eye and Ear, Boston, Massachusetts, USA
Harvard Medical School, Cambridge, Massachusetts, USA
E-mail: alex_hwang@meei.harvard.edu

Abstract

Avoiding person-to-person collisions is critical for visual field loss patients. Any intervention claiming to improve the safety of such patients should empirically demonstrate its efficacy. To design a VR mobility testing platform presenting multiple pedestrians, a distinction between colliding and non-colliding pedestrians must be clearly defined. We measured nine normally sighted subjects' collision envelopes (CE; an egocentric boundary distinguishing collision and non-collision) and found it changes based on the approaching pedestrian's bearing angle and speed. For person-to-person collision events for the VR mobility testing platform, non-colliding pedestrians should not evade the CE.

Introduction

Avoiding person-to-person (P2P) collisions, especially in heavily traveled areas such as busy shopping malls or transportation terminals/stations, is an everyday task frequently reported as a difficulty by patients with peripheral visual field loss [1-5]. A simulation-based analysis also identified it as a risk factor for such patients [6]. Any clinical intervention claiming to improve mobility performance should demonstrate its efficacy regarding collision detection and avoidance capability in P2P conditions, which directly leads to walking safety.

Various devices have been introduced to reduce risk, such as prism glasses [7-11] and head-mounted displays [12-14]. Although such interventions have shown their validity by measuring their visual field expansion in clinical conditions, those vision measures were often conducted with a stationary stimulus (e.g., detection of a moving target while fixating on a point over a simple background), lacking the complexity of visual stimulus motion experienced while walking, thus fail to show the efficacy of an intervention in more problem specific collision conditions.

To overcome this problem, obstacle courses have been used to measure one's mobility performance [15-22]. Although obstacle courses provide better face validity than visual field measures, most obstacle courses are only composed of stationary obstacles and let the subject walk through the obstacle course. Therefore, obstacle courses may be suitable for measuring the fitness of navigation and path following, but they do not measure the real-world collision risk posed to the patients or an intervention's impact on risky mobility situations such as P2P collisions [23]. It is well known that when patients walk with a cane, which can easily detect a possible collision with stationary obstacles on the floor, they make minimum collision in the obstacle courses [17, 21].

To measure the P2P collision risk, moving obstacles must be included in the obstacle courses. However, it is hard to implement in a real-world obstacle course because 1) deploying colliding pedestrians will increase the risk of physical collision and reduce the safety of participants, 2) controlling pedestrian path and collision timing and keeping the consistency for repeated executions will be very tricky, 3) modifying obstacle course configuration (e.g., path shape and pedestrians positioning) will be limited by physical space and take a long time. Therefore, a virtual obstacle course may be a better solution for the realistic mobility performance measure since it can resolve the problems of real-world obstacle courses mentioned above.

Since collision events will be simulated in a VR environment, no physical harm will be posed to the participants, the design of collision events can be precisely parameterized, and collision events can occur in any virtual environment. In addition, a virtual obstacle course conveniently affords positional tracking of the subject and target, making further analysis of collision detection and avoidance processes possible.

To measure one's collision risk quantitatively and reliably in a virtual obstacle course simulating heavy pedestrian traffic, subjects must be repeatedly exposed to dynamic situations where a P2P collision may (or may not) occur while multiple other pedestrians walk in various directions. No collision events should be included to reduce the priming effect. During the experiment, subjects must detect potential collision risks and take appropriate actions to avoid the collision, such as changing the walking path, slowing down, stopping until the approaching pedestrian passes by, or producing an auditory warning (e.g., "watch out"). The subject's performance measure should focus on how well and safely to avoid possible collisions. If it is for evaluation of an intervention, it should be measured with and without the intervention so that within-subject comparison is possible.

The successful development of such a testing platform depends on how well various dynamic events are designed with multiple pedestrians so that the distinction of apparent motion and looming between colliding and non-colliding pedestrians are clear enough, yet not obvious. Subjects should not misjudge non-colliding pedestrians as colliding or colliding pedestrians as non-colliding. Since this subject's perceptual error reduces the validity of the test, this kind of confusion should be removed or reduced as much as possible.

A pedestrian collision can be defined as an event where the following two conditions are met: 1) the subject's walking path intersects with another pedestrian's walking path, and 2) the subject and pedestrian arrive at the intersection simultaneously. The event can be considered non-colliding if any of those conditions are not met. However, the distinction between colliding and non-colliding events in the psychophysical experiment is more complex than the physical definition because the subject's visual judgment of collision may be affected by the perception of direction and speed of self-motion, of relative motion of other objects to self-motion, estimation of collision risk, etc.

The concept of collision envelope (CE or safety envelope) was introduced previously to measure the perceptual threshold for the subject's lateral safe passing margin [24-28]. Studies showed that people have an internal safety boundary larger than their physical width to avoid center-to-center collision and safely prevent partial contact with by-passing objects. In those studies, static human-sized objects appeared at a distance with a lateral offset for a brief time (1sec) and asked if the object would collide if subjects continued walking straight. In other words, it asked if the appeared object's width overlapped with the subject's perception of lateral safe passing margin. For example, it is like judging if one can pass a door without contacting the door frame.

Although those CE studies showed interesting results, such as a shifting of the CE center for homonymous hemianopia patients (i.e., loss of vision on the left or right side) while keeping the same CE width, those results have limited application to the highly dynamic walking scenarios where the colliding (and non-colliding) pedestrians may approach from various bearing angles (i.e., angle from walking direction).

If pedestrians are approaching from diagonal directions (i.e., the walking paths of the subject and pedestrian are not parallel), or if they are approaching at fast or slow speed (i.e., increased or reduced apparent risk in terms of consequence, respectively), is the CE affected by those factors? If it does, what change may occur to the CE? Previously, the safe passing distances for pedestrians approaching from various bearing angles were measured in a driving simulator that simulated virtual walking[11, 27] and demonstrated that a larger safety margin is needed for the pedestrians passing in front than those passing behind, which suggested a different safe passing distance may exist with the various bearing angle, but it was measured with poor resolution and did not formulate the full shape of the CE.

A parameter of interest in developing a virtual walking simulation for collision judgment/avoidance is how large a safe passing offset should be for pedestrians when they are supposed to pass by the subject so that the subject perceives it as non-colliding (non-risky) pedestrians. If the offsets are too large, detecting and judging potential collision becomes trivial. Thus, non-colliding pedestrians will not work as distractors. Also, if the offsets are too small, the subjects may perceive non-colliding pedestrians as possible collisions, resulting in too many false positive responses for potential collisions.

In this study, we measured normally sighted subjects' collision envelope during simulated slow and fast walking, where a virtual pedestrian approached from various bearing angles with lateral offsets (different passing distances). The measured normative 2D CE boundary can be used as a guideline for designing colliding and non-colliding pedestrians, where colliding pedestrians should be configured to invade the subject 2D CE while non-colliding pedestrians should not invade the 2D CE during virtual person-to-person collision event simulations.

Design of Pedestrians

Overall Geometry of Collision Event Design

The pedestrian collision events can have an infinite set of configurations based on the pedestrian's initial distance, walking speed, and initial bearing angle from the subject's walking path, etc. Therefore, we used a simple geometry collision model to simplify the event development.

Fig. 1 shows the geometry of a possible set of pedestrian collision events where the virtual avatar (subject) walks toward the assumed collision point (ACP) at a constant walking speed with a time-to-contact (TTC) of 5s. With a fixed TTC, we do not need to worry about the variable event duration. A pedestrian may appear at one of the bearing angle positions on the circle centered at the ACP with a radius of 5s of TTC of the subject's walking speed. Throughout the rest of the manuscript, a positive and negative bearing angle means the pedestrians are positioned on the right and left side of the subject's walking path, respectively.
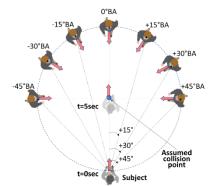

Figure 1: A schematic of collision events geometry. The subject is assumed to walk in a straight path at a constant speed. The assumed collision point can be determined based on the time-to-collision and the subject's walking speed. A pedestrian appears along the circle centered at the assumed collision point.

Notice that the initial appearing positions of the pedestrians with ±45° bearing angles are closer to the subject's initial position than other pedestrians, while the distance to the initial appearing positions of the pedestrians with 0° bearing angle (i.e., along the subject's walking path) is farthest.

This design simplifies the event configuration so that three parameters completely describe an event: 1) TTC, 2) the subject's walking speed, and 3) the pedestrian's initial bearing angle. This also sets the walking speed of all pedestrians to be uniform (i.e., same as the subject's walking speed) regardless of the pedestrian's initial position because their walking path length until making a collision will be the same.

Colliding Pedestrian

With the above event geometry, the colliding pedestrian will arrive at the ACP at the given TTC. Since the subject and pedestrian are assumed to walk on straight paths at a constant speed, both will arrive at the ACP simultaneously for a center-to-center collision. Note that in this colliding pedestrian design, the target pedestrian remains at the same bearing angle until the collision happens [28] (Fig. 2).

Non-Colliding Pedestrians

The non-colliding pedestrians are designed to initially appear at the same bearing angle position as the colliding pedestrians, but they are configured to arrive at a point on the front-parallel line of the approaching pedestrian passing the assumed collision point with an offset (Fig. 3). This means that the non-colliding pedestrians will be slightly off from the collision course. Thus, there will be no center-to-center collision.

If the initial bearing angle of the pedestrian is 0°, a positive lateral offset (offset>0m) and negative offset (offset<0m) result in a path rotated in a counterclockwise and clockwise direction from the center-to-center collision path (offset=0m).
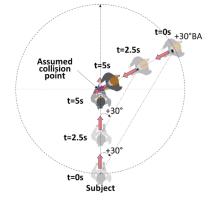
Figure 2: Modeling of a colliding pedestrian. The pedestrian is configured to walk toward the assumed collision point with the same walking speed as the subject. Both the subject and pedestrian will arrive at the collision point simultaneously, resulting in a collision. Note that the bearing angle of the colliding pedestrian remained the same throughout the event.

Note that when the pedestrian's initial bearing angle is larger than 0 (i.e., approaching the subject from the right side), a positive offset results in the pedestrian crossing in front of the subject's walking path, and a negative offset results in the pedestrian to pass behind the subject. This behavior will be reversed if the pedestrian's initial bearing angle is less than 0 (i.e., approaching the subject from the left side). Unlike colliding pedestrians, the non-colliding pedestrians' initial bearing angle regarding the subject's point of view will not be maintained during the walking. For example, as the subject approaches the ACP, the non-colliding pedestrians move toward the center of the visual field and then move to the outer eccentricity (crossing ahead) or move toward the outer eccentricity passing by) while their angular size increases (looming) monotonically. The looming of the non-colliding pedestrian is slightly faster than the colliding pedestrian because the pedestrian needs to walk farther than the colliding pedestrian for the same TTC.

As shown in Fig. 3, a non-colliding pedestrian is configured to pass one of the points (blue dots) on the front parallel line, passing the assumed collision point when the subject arrives at the assumed collision point. The lateral offsets can be either ±2m or ±1m. If the lateral offset is 0m, it is in the same condition as a colliding pedestrian.

Methods

Experiment Setup

The VR walking simulator experiment was developed using the Unity 3D game engine and ran on Windows 10 PC (Intel i5, 16G RAM) with NVidia GTX-1060 GPU.

Subjects were sitting at 50cm from a large TV (65"), which covers 104° horizontal and 81.5° vertical field of view (Fig.4). The Unity 3D's rendering camera field of view (FOV) was matched with the FOV of the TV from the viewing position to maintain the correct angular size of pedestrians and environment, which eliminate any perspective distortion caused by the angular size mismatch between rendering and display condition.

The virtual subject's eye height was set to 150cm to provide the perspective of the virtual walking (upright standing) on the screen while the subject was seated in the real world. Once the subject adjusted the seat height for their comfort, the table height was adjusted so that the center of the TV was aligned with the subject's eye level. Aligning the subject's viewpoint in the real world to the virtual camera position is necessary for distortion-free

viewing of the simulated virtual environment to avoid the distortion caused by the perspective mismatch.

Figure 4: Experimental setup. A large display (104°H ×81.5°V) is placed on a height-adjustable table to align the subject's eye level with the screen center. The rendering camera's field of view and display field of view were matched. Subjects were instructed to press a key if an approaching pedestrian appeared to bump into them.

Experiment Design

Subjects were instructed to "Press key A if the approaching pedestrian appears to bump into you. If the pedestrian is not bumping into you, press key B. Make the judgment as quickly as possible".

For all trials, the TTC was set to 5s. The pre- and post-event walking periods of 1s and 2sec, respectively, were added to each trial (a total of 8s walk per trial). These pre- and post-walk segments were added to give subjects time for preparation and resting before and after the measurement event.

For each trial, the subject's virtual walking speed was set to either 0.8m/s (1.8mph: slow walk) or 1.2m/s (2.7mph: fast walk), which makes the length of the subject's walking path to be 4m (~13ft) and 6m (~20ft) for given 5s TTC, respectively. The target pedestrian's initial bearing angle was set to be one among ±45°, ±30°, ±15°, and 0°. The passing offset was set to be one among ±1m (non-colliding), ±2m (non-colliding), and 0m (colliding).

Subjects completed a scenario containing 350 trails (2 walking speeds × 7 bearing angles × 5 passing offsets × 5 repetitions), which took around 50 minutes. Subjects were free to pause the experiment and take a break, if needed, during the scenario run.
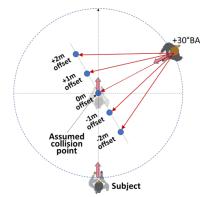

Figure 3: Modeling of non-colliding pedestrians. A pedestrian is configured to pass one of the points (blue dots) on the front-parallel line, passing the assumed collision point when the subject arrives at the assumed collision point. If the offset is non-zero, the pedestrian crosses in front of the subject or passes by the subject. If the offset value is 0, it results in collision.

The order of trials, including all combination of configuration factors, were randomly distributed over the scenario when the experiment was started so that each subject was exposed to a scenario with different trial orders.

Analysis of Safe-Passing Thresholds

Subject's binary responses to the approaching pedestrian (A: the pedestrian was perceived as colliding, and B: the pedestrian was perceived as non-colliding) with each passing offset was converted to the probability of true-positive response (i.e., a total number of positive responses divided by total repetitions per offset and bearing angle). Then, the probability values for the passing offsets were fitted to a logistic function.

$$f(x) = \frac{1}{1 + e^{-b(X-a)}}$$

A custom curve fitting algorithm was developed using dynamic programming to explore the best fitting parameters with the minimum total error within the known search ranges (e.g., [0 to 1] for the probability of collision judgment and [±2 to 1] for the lateral offset). For the left side of the responses, f(x) was fitted so that the model would have a higher probability of 'collision' responses for pedestrians approaching the subject's midline. If pedestrians cross with a large enough lateral offset, the probability of producing a 'collision' response becomes zero (too obvious). To fit the subject responses for the right-side passing pedestrians, -f(x) was fitted to find an internal psychophysical model of collision judgments.

Once a fitted logistic function is acquired, a 50% cutoff value is applied to compute the subject's collision judgment threshold. This process was applied to the pedestrians passing on the subject's left and right sides separately to get the passing offset for both sides (Fig. 5).
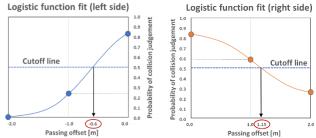

Figure 5: Example of logistic function fits to find the safe-passing thresholds. The subject's probability of positive responses (perceived as a colliding) was computed based on five repetitions for each offset (±1m, ±2m, and 0m) (blue and orange dots). A logistic function was fitted to each side (blue and orange lines). A cutoff value of 0.5 is applied to find the safe-passing threshold for the subject (blue dashed lines). This process was applied separately to the left and right sides of the subject's walking direction. In this example, the passing offsets for the left and right sides are -0.6m and +1.15m, respectively.

Note that for the pedestrians approaching from the same initial bearing angle, their lateral offset polarity decides which side of the subject the pedestrian passes by. For example, if the pedestrians with a positive initial bearing angle (i.e., +15° +30°, or +45°; approaching from the right side), the positive offset (i.e., +1m or +2m) makes the pedestrian passes by the right side of the subject (crossing behind), while the negative offset (i.e., -1m or -2m) makes the pedestrian passes by the left side of the subject (crossing ahead). These relative motion of the pedestrian to the subject's point of view are reversed when they are with negative initial bearing angles, where a positive offset makes the pedestrian passes by the left side of the subject, and

a negative offset makes the pedestrian passes by the right side of the subject.

The collision judgment thresholds for the pedestrians passing by the left and right sides are computed independently for each initial bearing angle. This threshold represents a subject's internal collision judgment criteria, where the subject is more likely to perceive an approaching pedestrian as a colliding pedestrian if the pedestrian passes by with a smaller offset than the threshold value. If the pedestrian passes by with an offset larger than the threshold, the subject will likely consider it a non-colliding pedestrian.

Participants

Nine normal vision subjects (42.1±20yrs, 6 males) participated in the study. No visually induced motion sickness was reported, and all participants completed the scenario. The study was approved by the Massachusetts Eye and Ear's Institutional Review Board and carried out in accordance with the ethical principles for medical research involving human subjects. All subjects gave written informed consent in accordance with the Declaration of Helsinki.

Results

Safe-Passing Thresholds

Fig. 6 shows the resulting safe-passing thresholds for all subjects regarding the pedestrians passing by on the subject's left and right side with various initial bearing angles when subjects were exposed to the slow (0.8m/s) and fast (1.2m/s) walking simulations. Each bar graph represents the safe-passing envelope with respect to the pedestrian approaching from each initial bearing angle. A longer bar indicates that a larger gap is needed to be perceived as a non-colliding pedestrian to be 'non-colliding' by the subjects.
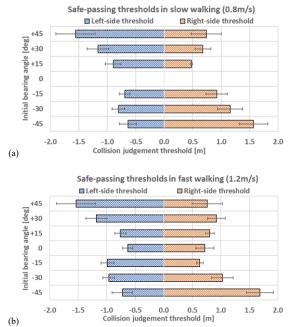

Figure 6: Safe-passing thresholds for pedestrians approaching from all initial bearing angles with (a) slow (0.8m/s) and (b) fast (1.2m/s) walking speeds for all subjects. A larger safe-passing envelope is required for pedestrians approaching from a larger initial bearing angle (outer eccentricity) than a smaller initial bearing angle (central eccentricity). Also, the safe-passing envelope (length of the bars) is larger for fast walking than for slow walking conditions. Note that in the slow-walking condition, subjects made no misjudgment for non-colliding pedestrians approaching from straight ahead, so the safe-passing threshold became zero, but the same subjects made a few misjudgments in the fast-walking condition, resulting in a non-zero threshold. Error bars indicate standard error.

5

A two-factor (bearing angle and walking speed) ANOVA with replication was applied to the size of the passing envelope (i.e., a sum of safe-passing thresholds for left and right sides) and found significant main effects on both factors, where the subjects required a larger passing threshold for the pedestrians with a larger initial bearing angle than smaller initial bearing angle ($F_{(6, 48)}=8.73$, $p<0.00$) and requires a larger threshold for the fast walking than slow walking conditions ($F_{(1, 8)}=4.08$, $p=0.046$). No significant interaction was found. Note that subjects made no misjudgment for those non-colliding pedestrians approaching from straight ahead as colliding in the slow walk condition, so the safe-passing threshold became zero. However, in the fast walk condition, some subjects misjudged the non-colliding pedestrians approaching from straight ahead as non-colliding, resulting in a non-zero threshold.

Response Time and Subject-Pedestrian Distance when Collision Judgement Was Made

The response time and the distance to the pedestrian when the collision judgment was made (i.e., key press), were analyzed for each initial bearing angle (Fig. 7). The results show that subjects judged a collision much earlier (~2.5s) than the actual collision (TTC of 5s). This indicates that collision judgments were made based on the estimation of where a potential collision may occur along the subject's walking path, and the subjects must have acquired enough information to predict oncoming pedestrians' moving direction and speed relative to the subject's motion, within 1s to 2s.
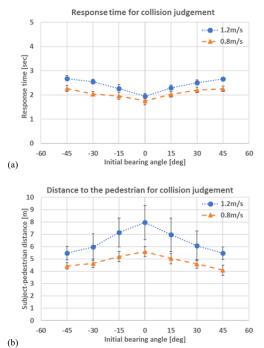

Figure 7: *Response time and subject's distance to the pedestrian when subjects responded. (a) A longer observation time was needed to make a collision judgment for fast walking than slow walking conditions, and the difference becomes larger for the pedestrians approaching from a large bearing angle than a small bearing angle. (b) When the distance to the pedestrian for collision judgment was considered, subjects made a judgment at father distance for fast walk conditions, and the distance differences were smaller for the pedestrian with a large bearing angle. Note that the initial distance between the subject and the pedestrian is larger for the fast walk condition than for the slow walk condition because all events are configured with the same time-to-collision parameter. Error bars indicate standard error.*

A two-factor (bearing angle and walking speed) ANOVA with replications was applied to the response time and found significant main effects where the subjects required more time to make a collision judgment (i.e., slower response time) in the fast walk condition than the slow walk condition ($F_{(1, 8)}=11.07$, $p<0.001$), and for the pedestrians with a larger initial bearing angle than smaller bearing angles ($F_{(6, 48)}=2.62$, $p=0.02$). No significant interaction was found.

The response time and the subject-pedestrian distance for collision judgment are not perfectly correlated because the pedestrian with a smaller bearing angle appears at a farther distance than the one with a larger bearing angle (see Fig. 1). Note that the difference between blue-circle (fast walking) and orange-triangle (slow walking) marker pairs becomes smaller as the bearing angle increases where an inversed trend is shown for the subject-to-pedestrian distance. This is because the initial distance between the subject and the pedestrian is farther for the fast walk condition than the slow walk condition, even for the same bearing angle pedestrians. All events were configured along the circle with a radius of the same TTC multiplied by the walking speed (see Fig. 1).

A two-factor (bearing angle and walking speed) ANOVA with replication was applied to the subject-to-pedestrian distance and found significant main effects on both factors. Subjects made a collision judgment at a significantly farther distance for the fast walk condition than slow walk condition ($F_{(1, 8)}=4.44$, $p<0.01$), and for the pedestrian approaching from central eccentricity than outer eccentricity ($F_{(6, 48)}=39.61$, $p<0.01$). No significant interaction was found.

2D Collision Envelope (2D-CE) during Walking

Since subjects made a judgment of collision (or no collision) that may occur at the ACP, the measured safe-passing envelopes (Fig. 6) can be radially arranged at the ACP to produce a 2D-CE (Fig. 8). For example, the safe-passing thresholds for the pedestrians with an initial bearing angle of ±45° were arranged along the vertical axis because such non-colliding pedestrians walk along the front-parallel line crossing the ACP. The safe passing envelopes for the pedestrians with an initial bearing angle of ±30° were arranged along the ±30° line from the vertical axis, crossing the ACP.

As expected, the shape of the 2D-CE was changed by the walking speeds, where the egocentric forward portion of the 2D-CE for the slow walk condition was wider than the rear portion during the slow walk condition. The shape of the 2D-CE was, in some sense, reversed during fast walk conditions (i.e., narrower forward portion than the rear portion). In both walking speed conditions, the forward portion stretched farther than the rear portion. However, the overall size of the 2D-CE is similar regardless of the walking speed.

These 2D-CEs indicate that when the subjects walk slowly, they try to secure more safety margins for the pedestrians crossing in front of the subjects' walking path. When the subjects walk fast, they try to secure more safety margins for the pedestrians crossing behind the subject's walking path. In both walking speeds, subjects put larger safety margins for the pedestrians approaching from the forward direction. Remember that the 2D-CE is positioned around the ACP estimated along the forward direction. Therefore, the forward portion of the 2D-CE is always ahead of the subject's current position, suggesting that the walking subjects estimated the possible collision by constant prediction.
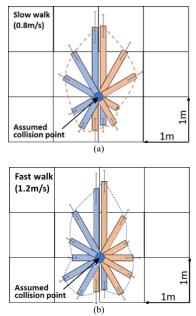
Figure 6: 2D collision envelopes (2D-CE) for (a) slow (0.8m/s) and (b) fast (1.2m/s) walking conditions. 2D-CEs were constructed by radially arranging individual safe-passing thresholds, shown in Fig. 7, at the assumed collision point. The shape of 2D-CE indicates the perceptual egocentric boundary for a predicted collision when the subjects arrive at the assumed collision point.

We assume the subject continuously computed and predicted a possible collision with an approaching pedestrian, which might occur at (or around) the ACP, based on perceived egocentric motion and visually estimated pedestrian motion in space. This 2D-CE shape change may be due to the fact that subjects usually bypass the other pedestrians in the fast-walking condition, so subjects may overestimate their walking speed (or underestimate the pedestrian walking speed) and thus expect to arrive at the ACP slightly earlier than the approaching pedestrian. So, they need to secure more safety space for the rear portion. An estimation of the opposite direction may exist for the slow-walking conditions, and the subjects may expect to arrive at the ACP slightly later than the pedestrians. So, the subjects try to secure more space on the forward portion.

Conclusions

In this study, we directly measured the shape of 2D-CE during walking. The subjects will perceive that there will be a collision if a pedestrian's walking path invades the 2D-CE in the future. The shape of the 2D collision envelope changes based on the subject's walking speed. Note that in our collision event design, the walking speed parameter applies to both the subject and pedestrian so that a light increase in the walking speed greatly increases the impact of the collision.

An interesting point of the measured 2D-CE is that most of the 2D-CE shape change due to the walking speeds changes occurred for the pedestrians approaching from ±15° or ±30° initial bearing angles (e.g., diagonal impacts), but not for the ones with ±45° initial bearing angles (e.g., side impacts). It may be related to how human subjects estimate the speed and direction of an approaching pedestrian. Subjects must rely more on looming information for pedestrians approaching the ACP diagonally because the bearing angle will be less visible at a far distance. For the side approaching, both looming and bearing angle shifts are clearly visible and can be utilized. Note that their bearing angle remains the same for colliding pedestrians, but for non-colliding pedestrians, the subject needs to keep monitoring if the bearing angle is changing. Since the diagonally moving pedestrian shows less lateral motion than the approaching pedestrian, the subject may have less confidence in their prediction for those pedestrians, resulting in more variations in 2D-CE for those pedestrians approaching the ACP diagonally than from the side.

Although it is hard to confirm why a subject's walking speed change induces such shape morphing in 2D-CE from our data, our data provides a convenient reference for designing non-colliding pedestrians that can be clearly distinguishable from the colliding pedestrians.

In our analysis, the safe-passing margin was decided by applying a 50% cutoff, which means that subjects perceive non-colliding pedestrians with a lateral offset at the threshold value may be misjudged as a colliding pedestrian half the times, indicating that this threshold value may not be sufficient for designing a non-pedestrian for a clear distinction. Therefore, to provide a clear distinction between colliding and non-colliding pedestrians, it will be more practical to apply a cutoff that is smaller than 50% (e.g., 25% or even 10% cutoff) to get a larger 2D-CE or double the safe-passing offset for a safe margin.

We implemented walking scenarios with multiple pedestrians based on such offsets and confirmed that it provides realistic complexity of busy shopping mall-like simulations, and subjects can clearly distinguish the colliding pedestrian from non-colliding pedestrians (see the demo video for multiple pedestrians in action).

Acknowledgments

References

[1] Turano KA, Geruschat DR, Stahl JW, and Massof RW. Perceived visual ability for independent mobility in persons with retinitis pigmentosa. Investigative Ophthalmology & Visual Science. 1999;40:865-77.

[2] Geruschat DR, and Turano, K. A. Connecting research on retinitis pigmentosa to the practice of orientation and mobility. Journal of Visual Impairment & Blindness. 2002;96:69–85.

[3] Sugawara T, Hagiwara A, Hiramatsu A, Ogata K, Mitamura Y, and Yamamoto S. Relationship between peripheral visual field loss and vision-related quality of life in patients with retinitis pigmentosa. Eye (Lond). 2010;24:535-9.

[4] Lisboa R, Chun YS, Zangwill LM, Weinreb RN, Rosen PN, Liebmann JM, … and Medeiros FA. Association between rates of binocular visual field loss and vision-related quality of life in patients with glaucoma. JAMA ophthalmology.131:486–94.

[5] Lovie-Kitchin J, Mainstone J, Robinson J, and Brown B. What areas of the visual field are important for mobility in low vision patients? . Clinical Vision Sciences. 1990;5:249–63.

[6] Peli E, Apfelbaum H, Berson EL, and Goldstein RB. The risk of pedestrian collisions with peripheral visual field loss. Journal of Vision. 2016;16:5.

[7] Peli E. Prentice Award Lecture: Peripheral Prisms for Visual Field Expansion: A Translational Journey. Optometry and Vision Science. 2020;In press.

[8] Somani S, Michael HB, and Markowitz SN. Visual field expansion in patients with retinitis pigmentosa. Canadian journal of ophthalmology. 2006;41:27-33.

[9] Jung JH and Peli E. Field Expansion for Acquired Monocular Vision Using a Multiplexing Prism. Optometry and Vision Science. 2018;95:814-28.

[10] Choi HJ, Peli E, Park M, and Jung JH. Design of 45∘ periscopic visual field expansion device for peripheral field loss. Optics Communications. 2020;454:124364.

[11] Qiu C, Jung JH, Tuccar-Burak M, Spano L, Goldstein R, and Peli E. Measuring pedestrian collision detection with peripheral field loss and the impact of peripheral prisms. Transl Vis Sci Technol. 2018;7:1-.

[12] Trese MG, Naheed W. Khan, Branham K, Conroy EB, and Moroi SE. Expansion of severely constricted visual field using Google Glass. Ophthalmic Surgery, Lasers and Imaging Retina. 2016;47:486-9.

[13] Ehrlich JR, Ojeda LV, Wicker D, Day S, Howson A, Lakshminarayanan V, and Moroi SE. Head-mounted display technology for low-vision rehabilitation and vision enhancement. American journal of ophthalmology. 2017;176:26-32.

[14] Sayed AM, Kashem R, Abdel-Mottaleb M, Roongpoovapatr V, Eleiwa TK, Abdel-Mottaleb M, Parrish II RK, and Abou-Shousha M. Toward Improving the Mobility of Patients with Peripheral Visual Field Defects with Novel Digital Spectacles. American journal of ophthalmology. 2019.

[15] Soong GP, Lovie-Kitchin JE, and Brown B. Does mobility performance of visually impaired adults improve immediately after orientation and mobility training? Optometry and Vision Science. 2001;78:657-66.

[16] Leat SJ and Lovie-Kitchin JE. Measuring mobility performance: experience gained in designing a mobility course. Clin Exp Optom. 2006;89:215-28.

[17] Fuhr PS, Liu L, and Kuyk TK. Relationships between feature search and mobility performance in persons with severe visual impairment. Optometry and Vision Science. 2007;84:393-400.

[18] Roentgen UR, Gelderblom GJ, and de Witte LP. The development of an indoor mobility course for the evaluation of electronic mobility aids for persons who are visually impaired. Assistive Technology. 2012;24:143-54.

[19] Patel I, Turano KA, Broman AT, Bandeen-Roche K, Munoz B, and West SK. Measures of visual function and percentage of preferred walking speed in older adults: the Salisbury Eye Evaluation Project. Invest Ophthalmol Vis Sci. 2006;47:65-71.

[20] Roentgen UR, Gelderblom GJ, and de Witte LP. User evaluation of two electronic mobility aids for persons who are visually impaired: A quasi-experimental study using a standardized mobility course. Assistive Technology. 2012;24:110-20.

[21] Zebehazy K, Zimmerman G, Bowers AR, Luo G and Peli E. Establishing Mobility Measures to Assess the Effectiveness of Night Vision Devices: Results of a Pilot Study. J Vis Imp Blind. 2005:99 (10) 663-670.

[22] Bowers AR, Luo G, Rensing NM. and Peli E. Evaluation of a prototype minified augmented-view device for patients with impaired night vision. Ophthal Physiol Opt, 2004:24: 296-312.

[23] Houston KE, Alex R. Bowers, Eli Peli, and Woods RL. Peripheral prisms improve obstacle detection during simulated walking for patients with left hemispatial neglect and hemianopia. Optometry and vision science: official publication of the American Academy of Optometry. 2018;95:795.

[24] Woods RL, Shieh JC, Bobrow L, Vora A, Barabas J, Goldstein RB, and Peli E. Perceived collision with an obstacle in a virtual environment. Investigative Ophthalmology & Visual Science. 2003;44:4321-.

[25] Luo G, Woods RL, and Peli E. Collision judgment when using an augmented-vision head-mounted display device. Investigative Ophthalmology & Visual Science. 2009;50:4509-15.

[26] Houston KE, Woods RL, Goldstein RB, Peli E, Luo G, and Bowers AR. Asymmetry in the collision judgments of people with homonymous field defects and left hemispatial neglect. Investigative Ophthalmology & Visual Science. 2015;56:4135-42.

[27] Feldstein IT, Felix M. Kölsch, and Konrad R. Impending collision judgment from an egocentric perspective in real and virtual environments: A review. Perception. 2019;48:769-95.

[28] Apfelbaum H, Pelah A, and Peli E. Heading assessment by "tunnel vision" patients and control subjects standing or walking in a virtual reality environment. ACM Trans Appl Percept. 2007;4:8.

[29] Jung JH, Castle R, Kurukuti NM, Manda S, and Peli E. Field expansion with multiplexing prism glasses improves pedestrian detection for acquired monocular vision. Transl Vis Sci Technol. 2020;9:35.

[30] Chardenon A, Montagne G, Buekers MJ, and Laurent M. The visual control of ball interception during human locomotion. Neurosci Lett. 2002;334:13-6.

Author Biography

Alex D. Hwang received BS in mechanical engineering from the University of Colorado Boulder (1999) and received MS (2003) and Ph.D. in computer science from the University of Massachusetts Boston (2010). Since then, he has worked at Schepens Eye Research Institute in Boston, where he is an Investigator and an Instructor of Ophthalmology at Harvard Medical School.

Jae-Hyun Jung received a BSc in Electrical Engineering from Pusan National University, Busan, Korea (2007), and a Ph.D. in Electrical Engineering from Seoul National University, Seoul, Korea (2012). He was appointed Assistant Scientist at Schepens Eye Research Institute of Mass Eye and Ear in Boston and an Assistant Professor of Ophthalmology at Harvard Medical School.

Alex Bowers received a Ph.D. Vision Rehabilitation Research from Glasgow Caledonian University, Scotland. Since then, she has been at the Schepens

Eye Research Institute, appointed as an Assistant Scientist and Associate Professor of Ophthalmology at Harvard Medical School.

Eli Peli *received a BSc and MSc in electrical engineering from Technician-Israel Institute of Technology (IIT), Haifa, Israel (1979), and OD from New England College of Optometry, Boston, MA (1983). Since then, he has been at the Schepens Eye Research Institute, where he is a Senior Scientist and the Moakley Scholar in Aging Eye Research, and Professor of Ophthalmology at Harvard Medical School.*